VERSITA

OPTO-ELECTRONICS REVIEW **19**(1), 61–65

DOI: 10.2478/s11772-010-0062-3

Investigation of influence of tilt angle on mode dispersion in step-index plastic optical fibers

M.S. KOVACEVIC*[1,2] and A. DJORDJEVICH[2]

[1]Faculty of Science, University of Kragujevac, 12 Domanovica Str., 34000 Kragujevac, Serbia
[2]MEEM Department, City University of Hong Kong, 83 Tat Chee Ave., Kowloon, Hong Kong

Effect of numerical aperture on mode dispersion and bandwidth is reported for commercially available step-index plastic optical fibers. For the first time, the functional relationship is given between dispersion and the "tilt-angle" describing the slant of the input/output face for a fiber terminated by a plane not perpendicular to the fiber axis. This tilt of a non-squarely terminated fiber may be intentional as in some biomedical spectroscopic sensors, or otherwise when exploiting the quick-interconnectivity potential of plastic fibers.

Keywords: mode dispersion, numerical aperture, tilt angle, step-index plastic optical fibers.

1. Introduction

Step index (SI) plastic optical fibers (POFs) have great potential for high-speed communication at short to medium distances. They have large core diameters and numerical apertures (0.2–0.8) that promote ease in system interconnectivity through simple but efficient coupling to light sources and detectors. POFs are flexible and remarkably resistant to mechanical damage and electromagnetic radiation. Main types of POFs, their manufacture, and possible present and expected future applications have been reported [1–3]. These studies have revealed great potential of plastic fibers to replace their glass counterparts and also copper cables in short-range data transfer applications.

Much research has focused on the computational simulation of fiber performance [4–10]. A number of methods of evaluating dispersion in optical fibers have been reported. Gloge has shown that dispersion in glass fibers depends on the fiber material and design parameters [11]. Dispersion causes temporal spreading of an input (pulse) signal, to an extent dependent on the signal bandwidth. This pulse broadening and the influence of launch conditions on dispersion have been investigated for large core step-index (SI) POFs [12] and graded-index fibers [13–18]. For example, geometric optics was used to obtain the pulse response of graded--index fibers [14] and a dispersion model of the fiber was presented based on its frequency response [15]. The dispersion in POFs has also been the subject of experimental investigations and computer simulations [19–21].

Effects are presented in this paper of the tilt-angle in angle-ended SI POFs (pertaining to slanted input/output faces) on mode dispersion in, and information-carrying capacity of, the fibers. For reference, pulse broadening is characterized in Sect. 2. How this broadening in SI POFs is influenced by numerical aperture is shown in Sect. 2. In Sect. 3, a model of angle-ended SI POF is presented. Calculation results are elaborated in Sect. 4. They show that the mode dispersion is significantly affected by the tilt-angle of the fiber input/output faces.

2. Background on mode dispersion in SI POF

Three main types of dispersion in optical fibers have been identified: mode dispersion (sometimes referred to as modal or ray dispersion), material dispersion, and waveguide dispersion. The transit time of modes of multimode optical fibers is different. This mode dispersion causes spreading of an optical impulse, with energy distributed among various modes, as it travels through the fiber. Although other pulse-spreading mechanisms may be present, mode dispersion is the dominant dispersion type in SI fibers including SI POFs, and it is the focus of this paper. Illustrated by examples, the textbook by Snyder and Love presents easy to understand fundamentals of dispersion in optical fibers [22].

Figure 1 shows two of many paths light can take within an SI POF. As their lengths differ, the corresponding rays launched simultaneously arrive to the fiber's output at different times, thus broadening the pulse they form. The ray propagating at $\theta_z = 0$ (Fig. 1) arrives first. The one at $\theta_z = \theta_{z(\max)}$ is the last to arrive. The corresponding propagation times t_{min} and t_{max} can be determined geometrically from Fig. 1

$$t_{\min} = \frac{L_1}{v} = \frac{L_1}{c/n_1} = L_1 \frac{n_1}{c}, \tag{1}$$

*e-mail: kruszka@ite.waw.pl

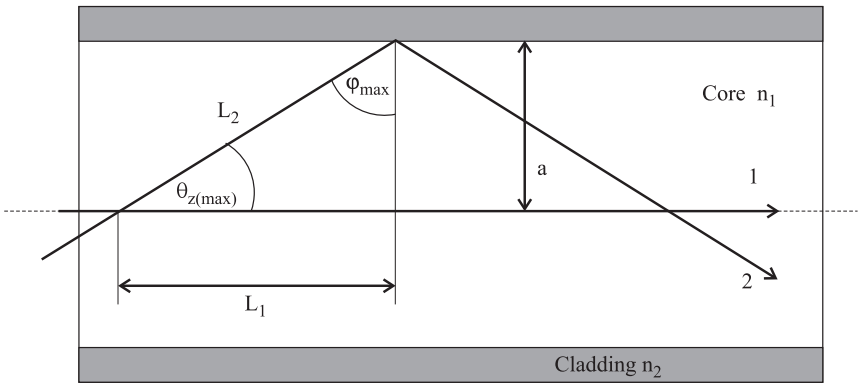

Fig. 1. Deriving transit-time difference.

and

$$t_{\max} = \frac{L_2}{v} = \frac{L_2}{c/n_1} = L_2 \frac{n_1}{c} = L_1 \frac{n_1}{c} \frac{1}{\sin\varphi_{\max}} = \frac{L_1}{c} \frac{n_1^2}{n_2}, \quad (2)$$

where n_1 and n_2 are the refractive indices of the core and cladding, respectively, and c is the velocity of light in free space. Simultaneously launched rays will therefore reach the output end over the time interval $\Delta\tau$ (also referred to as differential delay, Ref. 3)

$$\Delta\tau = t_{\max} - t_{\min} = \frac{n_1 L_1}{c}\left(\frac{n_1}{n_2} - 1\right). \quad (3)$$

Using the definition for numerical aperture

$$A_N = \sqrt{n_1^2 - n_2^2}, \quad (4)$$

the pulse spread or mode dispersion, $\Delta\tau$ in time, can be written in the form

$$\Delta\tau = \frac{L_1}{2cn_2} A_N^2. \quad (5)$$

This shows that the pulse spread is proportional to the square of the numerical aperture. From Eq. (3), for the weakly guiding fiber when $n_1 \cong n_2$, using $\Delta = (n_1 - n_2)/n_2$, it is

$$\Delta\tau \cong \frac{L_1 n_1}{c}\Delta \cong \frac{L_1 n_1 \theta_{z(\max)}}{2c}. \quad (6)$$

(It may be useful to note that by adding together $\Delta\tau$ of all individual segments typified in Fig. 1, each of the length L_1, Eqs. (3), (5), and (6) remain the same when $\Delta\tau$ represents the cumulative spread over the entire fiber length L). It is evident from Eq. (5) that the greater the fiber length, the greater the total pulse broadening becomes. Consequently, the time-gap between pulses in a series is reduced. Pulses "overflow" their intended time slots and overlap with adjacent ones. This limits the permissible frequency of the source pulses above which they overlap excessively for the receiver to discern them individually, leading to an increased bit error rate in communication systems. A commonly used criterion for the implied bandwidth limitation [24] is

$$\Delta\tau \le \frac{T}{4}, \quad (7)$$

where T is the bit duration. In terms of the bit rate $B\,(=1/T)$, Eq. (7) can be rewritten as

$$4\Delta\tau B \le 1. \quad (8)$$

The product of bandwidth and length characterizes the transmission capacity of the fiber. For the Gaussian-shaped pulses [3]

$$B \cdot L \approx \frac{0.44}{\Delta\tau} L, \quad (9)$$

where L represents the fiber's length. In POF systems, the limiting factor is usually the bandwidth of the fiber itself, which is created by modal dispersion. The following general relationship can be used as a rule for digital systems [3], maximum bit rate [Mbit/s] = 2 x bandwidth [MHz].

For a typical step-index POF, $n_1 = 1.492$ and $\Delta = (n_1 - n_2)/n_2 \approx 0.06$. Using Eq. (6), for $L_1 = 100$ m, a differential delay of $\Delta\tau \cong 30$ ns is obtained. Thus, in accordance with criteria of Eq. (7), two pulses separated by 100 ns at the input end may be resolvable at the end of a 100-m long fiber but not at the end of twice as long fiber as the delay would then be 60 ns, Fig. 2 [24].

Figure 3 shows how mode dispersion for an SI POF varies with numerical aperture according to Eq. (5).

The strong influence of the fiber numerical aperture on mode dispersion, and thereby bandwidth, is apparent in Fig. 3. If the fiber length is short enough to neglect mode coupling effects (as assumed in Fig. 3), then the mode dispersion is approximately proportional to the square of the fiber numerical aperture.

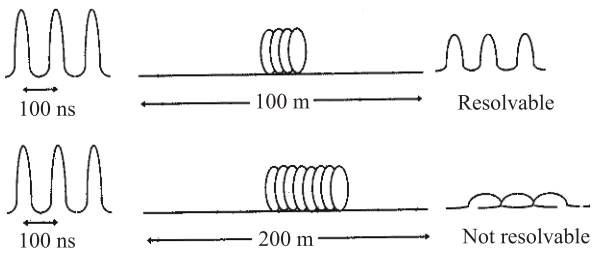

Fig. 2. Pulses separated by 100 ns at the input end may be resolvable at the output end of a 100-m, but not 200-m long fiber.

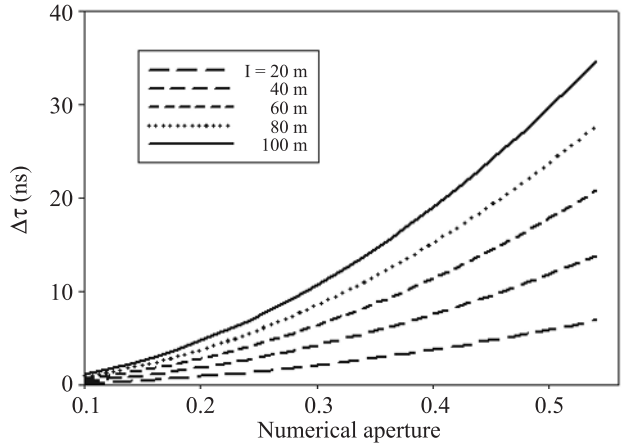

Fig. 3. Differential delay calculated as a function of numerical aperture.

Figure 4 shows how bandwidth drops with numerical aperture of fiber [as A_N^{-2} according to Eq. (5)]. From Eq. (9), $B \approx 0.44/\Delta\tau$. For the fiber length of 100 m, bandwidth of 15 MHz is obtained.

In general, the propagation characteristics at short distances are those of an ideal fiber: modes travel independently and dispersion grows linearly with a distance from the input end. As this distance increases, mode conversion and differential attenuation cause the far-field radiation pattern to evolve (it eventually becomes independent of launch conditions). Such transfer of energy between modes with different propagation constants tends to average propagation velocities and transit times. Consequently, the further increase in dispersion with distance from the input end is no longer a linear but only a square root function. This slows the bandwidth drop.

3. Modelling angle-ended SI POFs

Numerical aperture is a very important parameter of an optical fiber because it indicates the fiber capacity for accepting and guiding light. Fibers with a higher numerical aperture can accept more light (their bandwidth drops as light

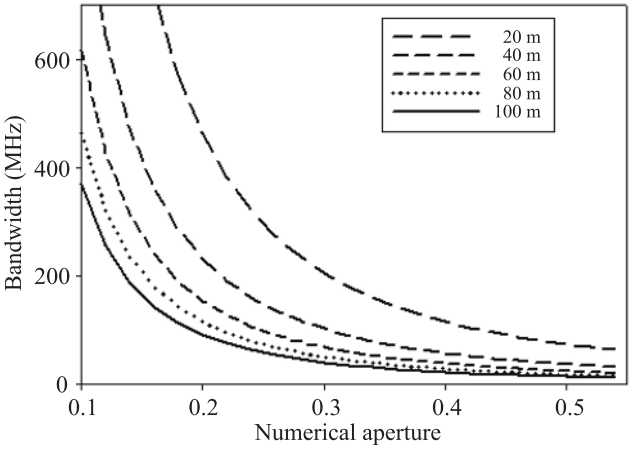

Fig. 4. Bandwidth calculated as a function of the numerical aperture.

launched with different incidence angles travels different path-length, known as modal dispersion, which limits the range of POF networks). The angle-ended fiber and its mathematical model were described in Ref. 23. Using the same formalism, we now extend the work presented in Ref. 23 in order to investigate the influence of the tilt-angle on modal dispersion in SI POF.

Optical fiber terminated squarely (Fig. 5) presents a circular face for coupling light to/from it.

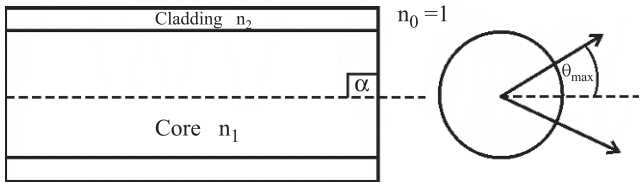

Fig. 5. A normally terminated fiber ($\alpha = 90°$).

The case when the fiber end-face is not perpendicular to the fiber axis is shown in Fig. 6 ($\alpha < 90°$). Such a fiber is called angle-ended fiber. The angle between the end face and cross-section of the fiber is tilt-angle, denoted by ε.

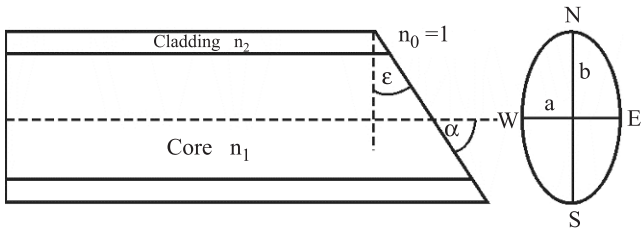

Fig. 6. An angle terminated fiber ($\alpha = 90°$).

The input/output end-face of the angle-ended fiber is an ellipse with its major axis b and the minor axis a shown in Fig. 6. Figure 7 shows ray trajectories for two critical meridional rays within a straight fiber, which refracted at the minor and major axis of the elliptical end-face. Refraction of the meridional ray that propagates in the plane through the minor axis a ("Ray 1" in Fig. 7) will, upon leaving the fiber, be at the angle θ_0 with respect to the normal, i.e., $\theta_0 \equiv \theta_{\max}$.

If the ray labelled as "Ray 2" is critical ray within the fiber, then its refracted angle with respect to the normal of the elliptical end-face will differ from θ_0. Following the formalism in Ref. 23, the "perturbed" numerical aperture in the case when the fiber is terminated with the tilt angle ε can be expressed as

$$A_N^{(t)} = \sin\theta_0' = \sin\frac{\arcsin[n_1\sin(\varepsilon+\theta_{z(\max)})]-\arcsin[n_1\sin(\varepsilon-\theta_{z(\max)})]}{2}. \quad (10)$$

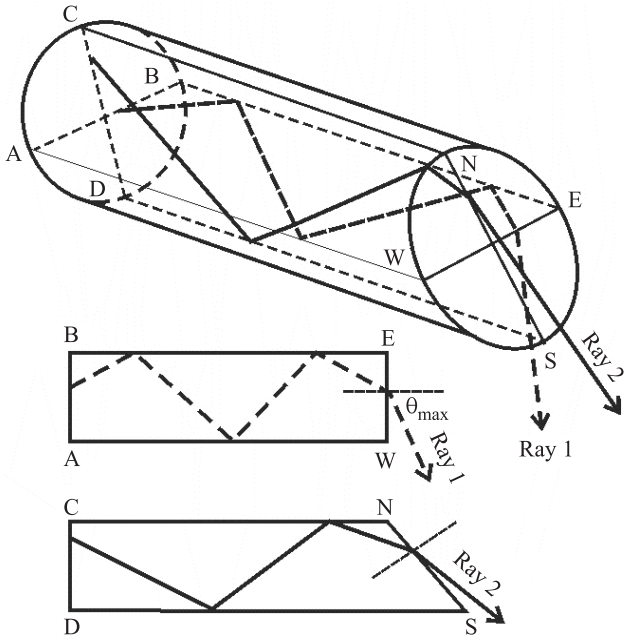

Fig. 7. Two critical rays in two meridional planes.

4. Simulation results and discussion

We have carried out computer simulation for the SI POF with a radius of 0.125 mm and refraction indexes of the core and cladding of 1.492 and 1.402, respectively. It can be observed that, for the fiber considered, the maximum value of the tilt angle $\varepsilon_{\max}$ is given by $n_1 \sin(\theta_z + \varepsilon_{\max}) = n_0$, which gives $\varepsilon_{\max} = 22°$.

The graph in Fig. 8 shows the mode dispersion of SI POF as a function of the fiber length for four different tilt-angles. The plots are obtained by Eqs. (5) and (10) assuming a uniform excitation and neglecting mode coupling. Linear dependence of the mode dispersion on fiber length is apparent. Moreover, the greater the magnitude of the tilt-angle, the greater the pulse spread. It can be observed that the time delay for a 100-m long fiber is 35 ns if the tilt-angle is $\varepsilon = 15°$. This delay is 30 ns in the absence of the tilt ($\varepsilon = 0°$). Thus, two pulses separated by, say, 100 ns at the input end would still be resolvable at the end of a 100-m long fiber.

The graph in Fig. 9 represents the bandwidth of SI POF as a function of fiber length for four values of the tilt-angle. The doted curve at the top is for the tilt-angle equal to zero. As expected, the bandwidth is a nonlinear function of fiber length. It can be observed that the fiber bandwidth drops as the tilt angle increases.

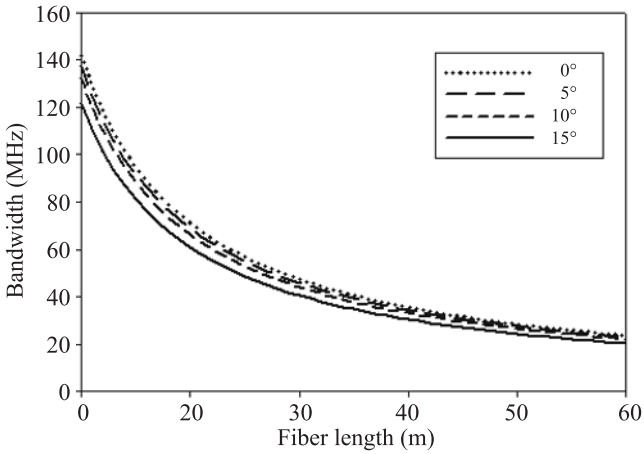

Fig. 9. Bandwidth of SI POF *vs.* fiber length for several tilt-angles.

For the same fiber, Fig. 10 shows how mode dispersion varies with the tilt-angle depending on the fiber length. It can be observed that this dependence is more pronounced and non-linear for larger lengths, becoming weaker and more linear for shorter fibers. We proposed the following approximation for the functions $\Delta\tau = f(\varepsilon)$ in Fig. 10

$$\Delta\tau = a + b\exp(c\varepsilon), \tag{11}$$

where a refers to the ray dispersion for $\varepsilon = 0$. For the POF used, the following values are obtained by curve fitting, $a \approx 0.32$ and $b \approx 0.17$.

The plots in Fig. 11 show the bandwidth drop as a function of the tilt angle in the case of an SI POF. The solid

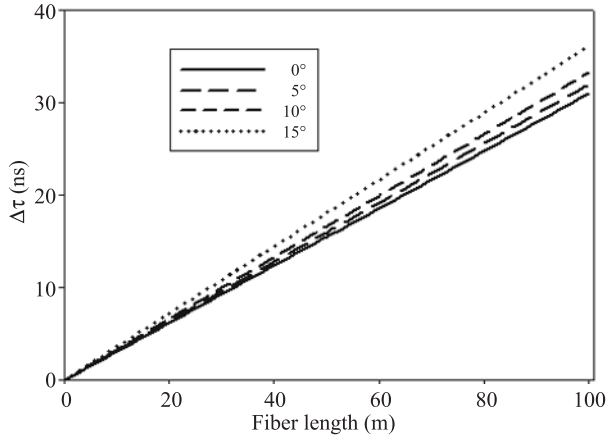

Fig. 8. Mode dispersion of SI POF as a function of fiber length for various values of tilt-angle.

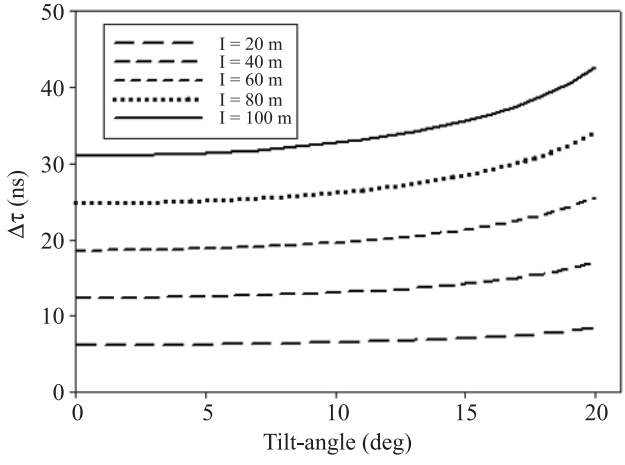

Fig. 10. Mode dispersion as a function of tilt-angle.

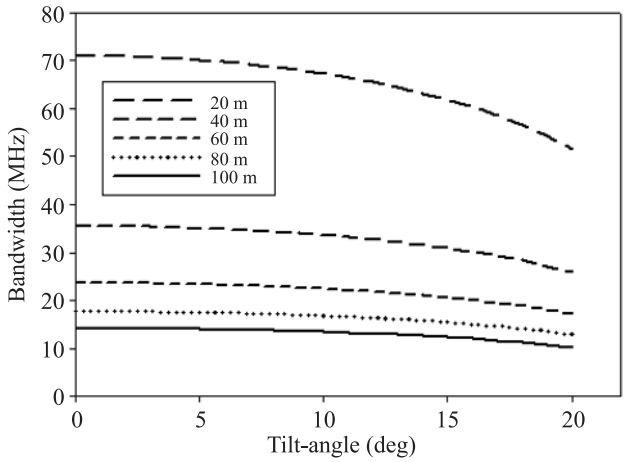

Fig. 11. Bandwidth *vs*. tilt-angle.

curve is for the longest fiber of 100 m. While, the bandwidth decrease was expected with increasing the fiber length, the same is apparent also with increasing the tilt-angle.

5. Conclusions

For non-squarely terminated step-index plastic optical fibers with a slanted input/output face, the influence is demonstrated of the corresponding tilt-angle of the face on the differential signal delay and fiber bandwidth. Such influence is routinely ignored or neglected by assuming squarely terminated fiber faces. Yet, the tilt angle is intentionally produced in some sensors, or can be a chance outcome when maximizing the quick-interconnectivity potential of plastic fibers, such as in data networks within buildings. The effects shown were modelled by exponential functions. The non-linear character of these functions is more apparent with greater tilt magnitudes. Mode dispersion and bandwidth change with numerical aperture are given as well.

Acknowledgements

The work described in this paper was supported by a grant from the City University of Hong Kong (SRG Project No.7002313) and in part by Serbian Ministry of Science, through Project No. 141023. The authors would like to express their gratitude for the financial support by the city of Kragujevac and the city mayor Mr V. Stevanovic.

References

1. J. Zubia and J. Arrue, "Plastic optics fibers: An introduction to their technological processes and applications", *Opt. Fiber Technol.* **7**, 1001–140 (2001).
2. C. Koeppen, R.F. Shi, W.D. Chen, and A. Garitto, "Properties of plastic optical fibers", *J. Opt. Soc. Am.* **B15**, 727–739 (1998).
3. W. Daum, J. Krauser, E.P. Zamzon, and O. Zeimann, *POF--Polymer Optical Fibers for Data Communication*, Springer--Verlag, Berlin, 2002.
4. *POF Modelling Theory, Measurement and Application*, edited by C.A. Bunge, and H. Poisel, Herstellung und Verlag: Books on Demand GmbH, Norderstedt, 2007.
5. M.S. Kovacevic, D. Nikezic, and A. Djordjevich, "Modelling of the loss and mode coupling due to an irregular core--cladding interface in step-index plastic optical fibers", *Appl. Opt.* **44**, 3898–3903 (2005).
6. A.F. Garito, J. Wnag, and R. Gao, "Effects of random perturbations in plastic optical fibers", *Science* **281**, 962–967 (1998).
7. G. Aldabaldetreku, G. Durana, J. Zubia, and J. Arrue, "Study of ray propagation mechanisms in multi step index optical fibers with use in computational methods", *J. Light. Technol.* **24**, 370–3778 (2006).
8. J. Arrue, J. Zubia, G. Fuster, and D. Kalymnios, "Light power behaviour when bending plastic optical fibres", *IEE P-0ptoelectron.* **145**, 313–318 (1998).
9. G. Durana, G. Aldabaldetreku, J. Zubia, J. Arrue, and C. Tanaka, "Coupling losses in perfluorinated multi-core polymer optical fibers", *Opt. Express* **16**, 7929–7942 (2008).
10. S. Savovic and A. Djordjevich, "Method for calculating the coupling coefficient in step-index optical fibers", *Appl. Opt.* **46**, 1477–1481 (2007).
11. G. Gloge, "Dispersion in weakly guiding fibers", *Appl. Opt.* **10**, 2442–2445 (1971).
12. P.D. Karim, "Multimode dispersion in step-index polymer optical fibers", *Proc. SPIE* **1799**, 57–66 (1992).
13. R. Olshansky and B.D. Keck, "Pulse broadening in graded--index optical fibers", *Appl. Opt.* **15**, 483–491 (1976).
14. F.K. Barrell and C. Pask, "Pulse dispersion in optical fibers of arbitrary refractive-index profile", *Appl. Opt.* **19**, 1298–1305 (1980).
15. G. Yabre, "Theoretical investigation on the dispersion of graded-index polymer optical fibers", *J. Light. Technol.* **18**, 869–877 (2000).
16. G. Yabre, "Comprehensive theory of dispersion in graded--index optical fibers", *IEEE J. Lightwave Technol.* **18**, 166–177 (2000).
17. K. Thyagarajan and B.P. Pal, "Modelling dispersion in optical fibers: applications to dispersion tailoring and dispersion compensation", *J. Opt. Fiber Comm. Rep.* **4**, 173–213 (2007).
18. T. Ishigure, "WKB method for POF modelling and optimization", *POF Modelling: Theory, Measurement, and Application*, edited by C.A. Bunge and H. Poisel, Herstellung und Verlag: Books on Demand GmbH, Norderstedt, 79–95 (2007).
19. C.A. Bunge, W Lieber, and D. Curticapen, "New aspects in bandwidth measurements considering the effects of DMD", *Opt. Laser Technol.* **39**, 61–67 (2007).
20. O. Ziemann, H. Poisel, A. Bachmann, and K.F. Klein, "Bandwidth measurements on SI- and Semi-GI-PCS", in *Proc. 13th POF Confer.*, pp. 251–254, Hong Kong, 2005.
21. T. Ishigure, M. Kano, and Y. Koike, "Which is a more serious factor to the bandwidth of GI POF: Differential mode attenuation or more coupling", *J. Lightwave Technol.* **18**, 959–965 (2000).
22. A. Snyder and J.D. Love, *Optical Waveguide Theory*, Champan and Hill, London, 1983.
23. M.S. Kovacevic, A. Djordjevuch, and D. Nikezic, "Effect of end-face tilt angle on numerical aperture for straight and bent plastic optical fibers", *Fiber Int. Opt.* **26**, 111–122 (2007).
24. A. Ghatak and K. Thyagarajan, *Introduction to Fiber Optics*, Cambridge University Press, 1998.